Universal Time-Dependent Control Scheme for Realizing Arbitrary Linear Bosonic Transformations

Ze-Liang Xiang,[1] Diego González Olivares,[2] Juan José García-Ripoll,[2] and Peter Rabl[3]
[1]School of Physics, Sun Yat-sen University, Guangzhou 510275, China
[2]Instituto de Física Fundamental IFF-PCSIC, Calle Serrano 113b, E-28006 Madrid, Spain
[3]Vienna Center for Quantum Science and Technology, Atominstitut, TU Wien, Stadionallee 2, 1020 Vienna, Austria

(Received 27 September 2022; accepted 13 January 2023; published 1 February 2023)

We study the implementation of arbitrary excitation-conserving linear transformations between two sets of N stationary bosonic modes, which are connected through a photonic quantum channel. By controlling the individual couplings between the modes and the channel, an initial N-partite quantum state in register A can be released as a multiphoton wave packet and, successively, be reabsorbed in register B. Here we prove that there exists a set of control pulses that implement this transfer with arbitrarily high fidelity and, simultaneously, realize a prespecified $N \times N$ unitary transformation between the two sets of modes. Moreover, we provide a numerical algorithm for constructing these control pulses and discuss the scaling and robustness of this protocol in terms of several illustrative examples. By being purely control-based and not relying on any adaptations of the underlying hardware, the presented scheme is extremely flexible and can find widespread applications, for example, for boson-sampling experiments, multiqubit state transfer protocols, or in continuous-variable quantum computing architectures.

DOI: 10.1103/PhysRevLett.130.050801

Linear unitary transformations between bosonic modes play an integral part in many quantum information processing applications. For example, by sending a multimode photonic Fock state through a network of linear optical elements—thereby implementing such a unitary transformation—the output distribution of the photons is exponentially hard to predict on a classical computer [1], but this boson-sampling problem can be simulated efficiently in a quantum experiment [2–9]. When combined with single-photon sources and detectors, the same unitary transformations can be used to realize a universal quantum computer according to the Knill-Laflamme-Milburn scheme [10,11]. Further, by encoding quantum information in continuous-variable degrees of freedom, one can benefit from efficient bosonic error correction schemes [12–15], which is currently explored in superconducting circuits [16–18] and trapped ion systems [19]. State transfer operations between such oscillator-encoded qubits require again the implementation of unitary transformations between distant bosonic modes.

In most applications, linear unitary transformations are realized by sending photons through a network of beam splitters and phase shifters [20], with a limited amount of tunability. In this Letter, we describe a universal protocol to achieve the same task through a controlled multiphoton emission and reabsorption process. The basic idea behind this approach is summarized in Fig. 1. Two quantum registers A and B, which each contain N bosonic modes, are connected by a unidirectional quantum channel. By controlling the coupling strength between the channel and each mode, a quantum state stored in register A is released as a propagating multiphoton wave packet and reabsorbed in register B. Here we demonstrate that, for any given $N \times N$ unitary matrix U, there exists a set of control pulses

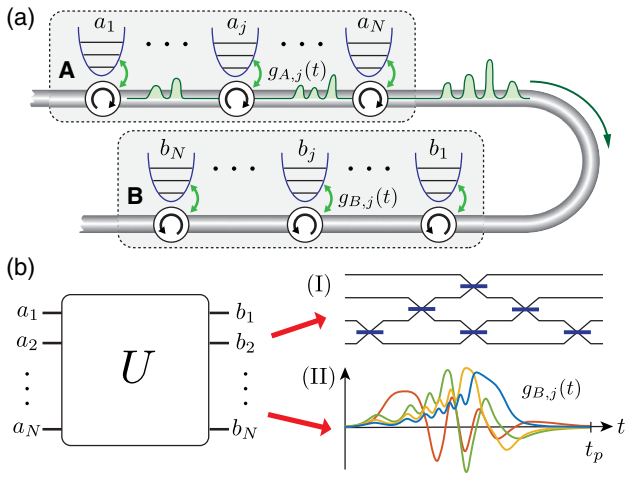

FIG. 1. (a) Sketch of the quantum network considered in this Letter. Two quantum registers A and B, each represented by N bosonic modes, are connected via a unidirectional waveguide. By controlling the couplings $g_{A,j}(t)$ and $g_{B,j}(t)$ between the modes and the waveguide, a multiphoton wave packet can be emitted from register A and successively be reabsorbed in register B. (b) A generic linear unitary transformation U between the modes, which is conventionally implemented by (I) sending photons through a network of $N(N-1)/2$ beam splitters, can be realized with our scheme in a time $t_p \sim N$ by (II) applying an appropriate set of control pulses.

such that (i) the reabsorption of the emitted photons can be achieved with arbitrarily high fidelity and (ii) the whole process implements the transformation

$$b_j(t_f) = \sum_{k=1}^{N} U_{jk} a_k(t_0). \tag{1}$$

Here the $a_k(t_0)$ are the bosonic annihilation operators for the modes of register A at the initial time t_0 and the $b_j(t_f)$ are the corresponding operators for the modes of register B at the final time t_f of the transfer. Moreover, we provide a numerical recipe for constructing the appropriate control pulses and show that even for completely random unitaries the overall protocol time, $t_p = t_f - t_0 \sim N$, only scales linearly with the number of modes. Therefore, the current approach offers an efficient and very flexible way to realize such transformations, where the targeted operation is fully specified by the shape of the control pulses and not by the network layout.

Quantum network dynamics.—For the following analysis, we focus on the quantum network in Fig. 1(a), where two sets of N bosonic modes in register A and register B are coupled to a unidirectional waveguide. For now we assume that all modes have the same frequency ω_0 and that they are coupled to the waveguide with tunable couplings $g_{A,j}(t)$ and $g_{B,j}(t)$, respectively, where $j = 1, \ldots, N$ labels the modes within each register. Various schemes for realizing such tunable couplings have already been demonstrated, both in the optical [21–24] and in the microwave regimes [25–33]. When combined with coherent circulators [34–39], chiral waveguides [40], or other types of directional couplers [41–43] a fully cascaded network, as assumed in this Letter, can be implemented.

Under the assumption that the spectrum of the waveguide is sufficiently broad and approximately linear, we can adiabatically eliminate the dynamics of the propagating photons and derive a set of cascaded quantum Langevin equations for the register modes [44,45]. In a frame rotating with ω_0, we obtain

$$\dot{c}_\mu(t) = -\frac{|g_\mu(t)|^2}{2} c_\mu(t) - g_\mu(t) f_{\mathrm{in},\mu}(t), \tag{2}$$

together with the input-output relations

$$f_{\mathrm{out},\mu}(t) = f_{\mathrm{in},\mu}(t) + g_\mu^*(t) c_\mu(t). \tag{3}$$

Here, the index μ runs over all $2N$ modes and we have made the identifications $c_\mu \equiv a_\mu$ and $g_\mu \equiv g_{A,\mu}$ for $\mu = 1, \ldots, N$ and $c_\mu \equiv b_{\mu-N}$ and $g_\mu \equiv g_{B,\mu-N}$ for $\mu = N+1, \ldots, 2N$. The in field $f_{\mathrm{in},1}(t) \equiv f_{\mathrm{in}}(t)$ is a δ-correlated noise operator, which satisfies $[f_{\mathrm{in}}(t), f_{\mathrm{in}}^\dagger(t')] = \delta(t-t')$. All other in fields are determined by the relation $f_{\mathrm{in},\mu}(t) = f_{\mathrm{out},\mu-1}(t)$, which captures the directional nature of the quantum channel. By iterating this relation and adopting a vector notation, $\vec{c} = (c_1, \ldots, c_{2N})^T$ and $\vec{g} = (g_1, \ldots, g_{2N})^T$, we obtain

$$\dot{\vec{c}}(t) = -\mathcal{M}(t)\vec{c}(t) - \vec{g}(t) f_{\mathrm{in}}(t), \tag{4}$$

where $\mathcal{M}_{\mu\nu}(t) = g_\mu(t) g_\nu^*(t) \Theta(\mu - \nu)$ and $\Theta(x)$ is the Heaviside function. Unless stated otherwise, we express time in units of $\gamma_{\max}^{-1}$, where $\gamma_{\max}$ denotes the maximal decay rate into the channel and depends on the specific physical implementation. With this convention, the couplings $g_\mu(t)$ are complex numbers and constrained to $|g_\mu(t)| \leq 1$. A detailed derivation of Eq. (4) can be found in the Supplemental Material [46].

The general solution of Eq. (4) can be written as

$$\vec{c}(t) = \mathcal{G}(t, t_0)\vec{c}(t_0) - \int_{t_0}^{t} ds\, \mathcal{G}(t, s)\vec{g}(s) f_{\mathrm{in}}(s), \tag{5}$$

where the Green's function $\mathcal{G}(t, t_0)$ obeys $\partial_t \mathcal{G}(t, t_0) = -\mathcal{M}(t)\mathcal{G}(t, t_0)$ and $\mathcal{G}(t_0, t_0) = \mathbb{1}_{2N}$. The cascaded structure imposed by the unidirectional waveguide implies that both $\mathcal{M}$ and $\mathcal{G}$ have a lower-triangular form, i.e., $\mathcal{M}_{\mu\nu}, \mathcal{G}_{\mu\nu} = 0$ for $\mu < \nu$. Moreover, each row μ of these matrices only depends on the couplings $g_\nu(t)$ associated with that and previous modes $\nu \leq \mu$. This allows us to write the Green's function as

$$\mathcal{G} = \begin{pmatrix} G_{AA} & 0 \\ G_{BA} & G_{BB} \end{pmatrix} \to \begin{pmatrix} 0 & 0 \\ U & 0 \end{pmatrix}, \tag{6}$$

where the expression to the right indicates the targeted evolution at $t = t_f$, as specified in Eq. (1).

Control pulses.—To realize the desired dynamics, we first choose a set of pulse shapes for the couplings $g_{A,j}(t)$ in register A. These pulses do not have to be of any specific shape, but they must be mutually overlapping and satisfy [46]

$$\int_{t_0}^{t_f} ds |g_{A,j}(s)|^2 \gg 1. \tag{7}$$

This condition ensures that all initial excitations in register A decay into the waveguide and $G_{AA}(t_f, t_0) \simeq 0$ up to exponentially small corrections.

Next, we must identify a set of control pulses $g_{B,j}(t)$, which achieve the nontrivial part of the dynamics, $G_{BA}(t_f, t_0) \to U$. To do so, we assume for now that the whole network is initially prepared in the single excitation state $|\psi_\ell\rangle = \Psi_\ell^\dagger |\mathrm{vac}\rangle$, where $|\mathrm{vac}\rangle$ is the vacuum state and $\Psi_\ell = \sum_{k=1}^{N} U_{\ell k} a_k(t_0)$. We then define the amplitudes $F_{j,\ell}(t, t_0) = \langle \mathrm{vac} | f_{\mathrm{out},N+j}(t) | \psi_\ell \rangle$, which represent the field in the channel right after the jth mode of register B. We obtain

$$F_{j,\ell}(t, t_0) = \sum_{k=1}^{N+j} g_k^*(t) [\mathcal{G}(t, t_0)\mathcal{U}^\dagger]_{k,\ell}, \tag{8}$$

where $\mathcal{U} = \mathrm{diag}(U, 0_N)$ is a block-diagonal matrix.

According to Eq. (1), the excitation created by $\Psi_\ell^\dagger$ is mapped onto the corresponding excitation of mode b_ℓ in register B. To achieve this mapping, during the whole protocol, the photon emitted from state $|\psi_\ell\rangle$ must not propagate beyond the ℓth node of register B, as otherwise it would be impossible to recapture it at a later time. Therefore, a necessary requirement for a perfect transfer is that the dark state condition $F_{\ell,\ell}(t,t_0)=0$ is satisfied for all times $t\in[t_0,t_f]$, or equivalently,

$$g_{B,\ell}^*(t)[\mathcal{G}(t,t_0)\mathcal{U}^\dagger]_{N+\ell,\ell}=-F_{\ell-1,\ell}(t,t_0). \tag{9}$$

For $N=1$ and $U=1$, Eq. (9) reduces to the dark-state condition employed for identifying control pulses for single-mode quantum state transfer schemes [33,50–55] (see also Ref. [56] for a preliminary extension to multimode setups). In the Supplemental Material [46], we show that satisfying this generalized set of dark-state conditions for all $\ell=1,\ldots,N$ is not only necessary, but also sufficient to obtain $G_{BA}(t_f,t_0)\simeq U$ and $G_{BB}(t_f,t_0)\simeq 0$ for sufficiently long t_f. Moreover, we show that the implicit equation for $g_{B,\ell}(t)$ in Eq. (9) can be converted into the following recursive expression:

$$g_{B,\ell}(t)=\frac{F_{\ell-1,\ell}^*(t,t_0)}{\sqrt{\int_{t_0}^t ds|F_{\ell-1,\ell}(s,t_0)|^2}}. \tag{10}$$

Because of the cascaded structure of $\mathcal{G}$, the amplitudes $F_{\ell-1,\ell}(t,t_0)$ depend on the known control pulses $g_{A,j}(t)$ and on the previously obtained pulses $g_{B,j}(t)$ for $j<\ell$ only. Therefore, Eq. (10) can be iteratively applied to compute all control pulses $g_{B,j}(t)$ for register B.

Equation (10) proves the existence of a solution to our control problem by an explicit construction of the coupling pulses, which is the main result of this Letter. We still need to show, however, that this formal result does not lead to solutions that violate the constraints $|g_j(t)|^2\le 1$, are unbounded in time, or otherwise unphysical. In the following, we achieve this conclusion by simply applying the protocol for engineering generic $N\times N$ unitary transformations. This approach will also allow us to deduce the scaling and the robustness of the protocol under realistic conditions.

Two-by-two unitaries.—In a first step, we illustrate the application of the protocol for the simplest nontrivial scenario, $N=2$, shown in Fig. 2(a). For this setup, we consider the four unitary operations

$$U_T=\begin{pmatrix}1&0\\0&1\end{pmatrix},\qquad U_S=\begin{pmatrix}0&1\\1&0\end{pmatrix},$$
$$U_H=\frac{1}{\sqrt{2}}\begin{pmatrix}1&1\\1&-1\end{pmatrix},\qquad U_C=\frac{1}{\sqrt{2}}\begin{pmatrix}1&i\\i&1\end{pmatrix}. \tag{11}$$

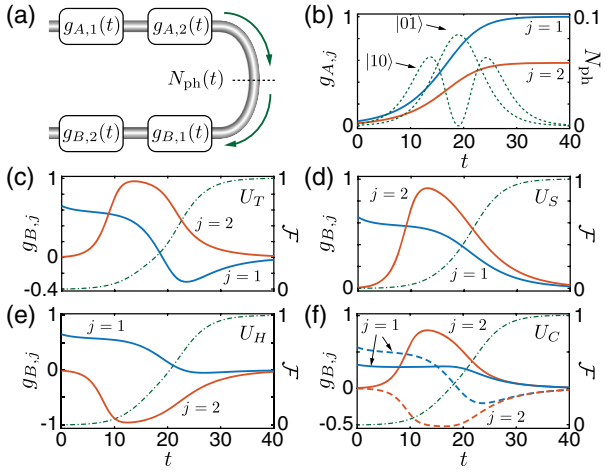

FIG. 2. (a) Sketch of the setup for implementing unitary operations between $N=2$ modes. (b) Shape of the control pulses $g_{A,j}(t)$ as specified in Eq. (12) and for the parameters $t_c=19$, $\delta=2$, and $\tau=1$. The dotted lines show the shape of the photon wave packet released from register A, $N_{\rm ph}(t)=|\langle{\rm vac}|f_{{\rm out},2}(t)|\psi_0\rangle|^2$, for different initial states $|\psi_0\rangle=|10\rangle$ and $|\psi_0\rangle=|01\rangle$. (c)–(f) Shapes of the optimal control pulses $g_{B,j}(t)$ for the unitaries (c) U_T, (d) U_S, (e) U_H, and (f) U_C. In all plots, the dash-dotted lines show the fidelity $\mathcal{F}$. (f) The solid lines represent the real part and the dashed lines the imaginary parts of the control pulses.

Here, U_T corresponds to a simple state transfer between the two registers, U_S additionally swaps the two modes, and the Hadamard operation U_H and the unitary U_C create superpositions between the modes with real and complex coefficients.

To calculate the control pulses for realizing each unitary, we set $t_0=0$ and fix the control pulses $g_{A,j}(t)$ to be of the form

$$g_{A,j}(t)=\frac{\eta_j}{\sqrt{e^{(t_c-t)/\tau}+1}},\qquad \eta_j=\sqrt{\frac{1+(N-j)\delta}{1+(N-1)\delta}}. \tag{12}$$

The parameters δ, t_c, and τ can be used to optimize the protocol for a given application, but none of the following findings depend crucially on this specific pulse shape nor on a specific set of parameters. The pulses $g_{A,j}(t)$ used in the following examples are depicted in Fig. 2(b).

Given $g_{A,j}(t)$ and U, we iteratively solve Eq. (10) numerically to obtain the control pulses $g_{B,j}(t)$ and evaluate the fidelity of the operation [57,58]

$$\mathcal{F}(t)=\frac{|{\rm Tr}\{U^\dagger G_{BA}(t,t_0)\}|^2+{\rm Tr}\{G_{BA}^\dagger(t,t_0)G_{BA}(t,t_0)\}}{N(N+1)}. \tag{13}$$

It reaches a value of $\mathcal{F}(t_f)\simeq 1$, if the protocol was successful. For the examples in Eq. (11), the resulting pulse shapes and fidelities are plotted in Figs. 2(c)–2(f).

We see that in all cases the algorithm provides the correct control pulses and the unitary transformation is implemented with close to unit fidelity, as long as the protocol time $t_p = t_f - t_0$ is long enough. We emphasize that, while the shape of the wave packet released from register A depends on the initial quantum state [see Fig. 2(b)], the implemented unitary U is independent of this state.

Scalability.—Using the construct from Ref. [20], a sequential combination of $\mathcal{O}(N^2)$ of the 2×2 unitary operations demonstrated above is sufficient to recreate any possible $N \times N$ unitary transformation U in a time $t_p \sim \mathcal{O}(N^2)$. This strategy is usually employed for implementing bosonic unitaries with photons or also atoms [59,60]. However, in the current approach, already in a single run, each of the emitted photons interacts with multiple modes in register B. This intrinsic parallelization allows us to improve over the scheme by Reck *et al.* [20] and obtain protocol times that only scale linearly with the number of modes, $t_p \sim \mathcal{O}(N)$.

To demonstrate this scaling, we numerically evaluate the minimal protocol time $t_{\min}$ required to implement a given $N \times N$ unitary with a fidelity of $\mathcal{F} \geq 0.99$. Specifically, we compare the implementation of the N-mode state-transfer operation $U_T(N) = \mathbb{1}_N$, the N-dimensional Hadamard transformation $U_H(N)$, and generic complex unitaries $U_R(N)$ with randomly drawn matrix elements. The results are summarized in Fig. 3(a) and demonstrate that the protocol works perfectly even for a large number of modes and for arbitrary classes of unitaries. As an illustrative example, Fig. 3(b) shows the control pulses $g_{B,j}(t)$ for $U_R(N = 8)$ and qualitatively similar pulse shapes are obtained for other unitaries as well. See the Supplemental Material [46] for further details about the numerical procedure that has been used to obtain these results.

The key observation from Fig. 3(a) is that $t_{\min} \sim N$ scales only linearly with the number of modes, independent of the specific properties of U. This scaling can be roughly understood as follows. Because the maximal coupling strength is bounded, $|g_j(t)| \leq \sqrt{\gamma_{\max}}$, the local modes can emit or absorb photons only on timescales longer than $\gamma_{\max}^{-1}$. Therefore, in order to emit (absorb) photons into (from) N spatiotemporally distinct modes, the total pulse duration must increase proportionally to N. The prefactor for this scaling is the same for all the tested unitaries, but it is still a factor of ~ 3 higher than what one would obtain from implementing N times a single-mode transfer. We attribute this overhead to the nonoptimal choice of control pulses $g_{A,j}(t)$ in Eq. (12). Indeed, for the transfer unitary $U_T(N)$, a substantial reduction of the protocol times can already be obtained by optimizing the parameter δ [46]. This suggests that also for other unitaries, a similar improvement of the scaling prefactor can be achieved by using other shapes for the control pulses in register A.

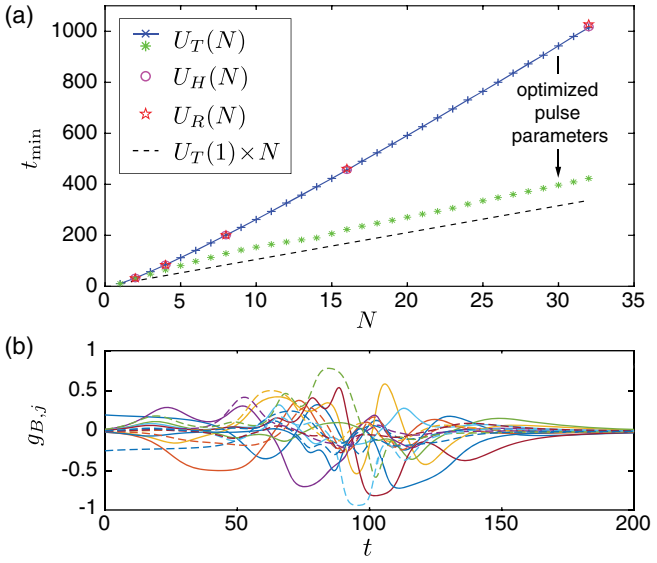

FIG. 3. (a) Scaling of the minimal protocol time $t_{\min}$ for implementing different classes of $N \times N$ unitaries with a fidelity $\mathcal{F} \geq 0.99$. Here, $U_T(N) \equiv \mathbb{1}_N$ is the state-transfer operation, $U_H(N)$ is the N-dimensional Hadamard transformation, and $U_R(N)$ is a random unitary $N \times N$ matrix. In all cases, the pulses $g_{A,j}(t)$ are specified in Eq. (12) with $\delta = 2$ and $\tau = 1$. The results marked by stars show the minimal protocol time for $U_T(N)$ for an optimized parameter δ. (b) Illustration of the numerically constructed control pulses $g_{B,j}(t)$ for the example $U_R(N = 8)$. The real and imaginary parts are shown by the solid and dashed lines, respectively. See the Supplemental Material [46] for additional details.

Imperfections.—For tunable couplers based on Raman or parametric driving schemes [24,31,33,43], the complex couplings $g_\mu(t) \sim \Omega_\mu(t)$ are directly proportional to the computer-generated amplitudes of the driving fields, but in practice experimental uncertainties lead to deviations from this exact relation and $g_\mu(t) = g_\mu(t)|_{\text{id}} + \delta g_\mu(t)$. To evaluate the impact of such pulse distortions, we assume

$$\delta g_\mu(t) = \sqrt{\varepsilon\Omega} \int_{-\infty}^{t} ds\, e^{-\Omega(t-s)/2} \xi_\mu(s), \tag{14}$$

where the $\xi_\mu(t)$ are independent white noise processes with $\langle \xi_\mu(t)\xi_\nu(t')\rangle = \delta_{\mu\nu}\delta(t-t')$, and ε and Ω determine the strength and the frequency range of the pulse distortion. From the simulations in Fig. 4(a), we find that the protocol is surprisingly robust with respect to pulse distortions. The infidelity $1 - \mathcal{F}$ scales sublinearly with the strength of the noise for rather high values of ε and fluctuations that are faster than $\gamma_{\max}^{-1}$ are further suppressed. Importantly, as shown in Fig. 4(b), the fidelity of the operation also does not degrade significantly when the number of modes is increased and again a rather weak dependence on N is observed.

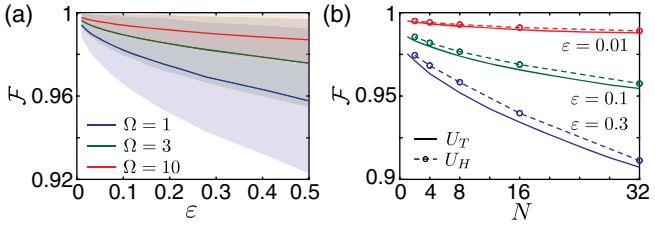

FIG. 4. Fidelity of the unitary transformation in the presence of pulse imperfections $\delta g_j(t)$ as defined in Eq. (14). (a) Scaling of the fidelity for the transformation $U_H(N=4)$ as a function of the strength of the noise ε and for different bandwidths Ω. The solid lines show the fidelity averaged over 10^4 noise realizations, with a standard deviation indicated by the shaded areas. (b) Dependence of the fidelity (averaged over 400 noise realizations) on the number of modes N for different strengths of the noise and for $\Omega = 1$. The solid and the dashed lines show the results as obtained for the state-transfer unitary $U_T(N)$ and for the Hadamard transformation $U_H(N)$, respectively.

In [46] we consider also other types of imperfections and show, first of all, that the protocol works equally well for nonidentical modes with frequencies $\omega_\mu = \omega_0 + \Delta_\mu$, even for detunings $\Delta_\mu \sim \gamma_{\max}$. Therefore, no precise fine-tuning of the local modes is required. Further, the linearity of the transformation makes the protocol insensitive to input noise, such as residual thermal excitations in the channel [54,55]. The effect of losses, however, reduces the fidelity of the ideal operation $\mathcal{F}_{\rm id}$ to [46]

$$\mathcal{F} \approx \mathcal{F}_{\rm id} e^{-\gamma t_p}(1-p_{\rm ch})(1-p_{\circlearrowleft})^{2N}. \tag{15}$$

Here, γ is the bare decay rate of the local mode, $p_{\rm ch}$ is the photon loss probability in the channel connecting register A and register B, and $p_{\circlearrowleft}$ is the transmission loss of a single circulator or nonreciprocal coupler. While for large N, Eq. (15) places stringent coherence requirements on all network components, it does not reveal any unexpected scalings that depend specifically on the current protocol or on the choice of the unitary transformation. Note, that $\mathcal{F}$ refers to the fidelity of the unitary transformation, as defined in Eq. (13). The fidelity of the transformed multiphoton state depends in a more complicated way on the initial photon numbers in each mode (see, for example, Ref. [54] for the case $N = 1$).

Conclusions.—In summary, we have presented a universal protocol for implementing excitation-conserving linear unitary transformations between N bosonic modes, where, instead of sending photons through a fixed network of beam splitters and phase shifters, the transformation is implemented through a multiphoton emission and reabsorption process. Therefore, arbitrary unitaries can be realized by simply changing the control pulses and without changing the network configuration. The protocol is robust with respect to the main sources of imperfections and, even for very complex unitaries, the protocol time only increases linearly with the number of modes.

While the protocol can be implemented with various physical platforms, we envision important near-term applications in the context of circuit QED, where high-fidelity directional couplers and other network components are currently developed [46]. Here, the protocol can be used for parallel state-transfer and entanglement distribution schemes or, when combined with local nonlinearities, for large-scale quantum computing architectures based on continuous-variable-encoded qubits.

This work was supported by the European Union's Horizon 2020 research and innovation program under Grant Agreement No. 899354 (SuperQuLAN), the National Natural Science Foundation of China (Grant No. 11874432), the National Key R&D Program of China (Grant No. 2019YFA0308200), Proyecto Sinérgico CAM 2020 Y2020/TCS-6545 (NanoQuCo-CM), and the CSIC Interdisciplinary Thematic Platform (PTI+) on Quantum Technologies (PTI-QTEP+).

[1] S. Aaronson and A. Arkhipov, The computational complexity of linear optics, Theory Comput. **9**, 143 (2013).
[2] J. B. Spring, B. J. Metcalf, P. C. Humphreys, W. S. Kolthammer, X.-M. Jin, M. Barbieri, A. Datta, N. Thomas-Peter, N. K. Langford, D. Kundys *et al.*, Boson sampling on a photonic chip, Science **339**, 798 (2013).
[3] M. A. Broome, A. Fedrizzi, S. Rahimi-Keshari, J. Dove, S. Aaronson, T. C. Ralph, and A. G. White, Photonic boson sampling in a tunable circuit, Science **339**, 794 (2013).
[4] M. Tillmann, B. Dakic, R. Heilmann, S. Nolte, A. Szameit, and P. Walther, Experimental boson sampling, Nat. Photonics **7**, 540 (2013).
[5] J. Carolan, J. D. A. Meinecke, P. J. Shadbolt, N. J. Russell, N. Ismail, K. Wörhoff, T. Rudolph, M. G. Thompson, J. L. O'Brien, J. C. F. Matthews, and A. Laing, On the experimental verification of quantum complexity in linear optics, Nat. Photonics **8**, 621 (2014).
[6] N. Spagnolo, C. Vitelli, M. Bentivegna, D. J. Brod, A. Crespi, F. Flamini, S. Giacomini, G. Milani, R. Ramponi, P. Mataloni, R. Osellame, E. F. Galvao, and F. Sciarrino, Experimental validation of photonic boson sampling, Nat. Photonics **8**, 615 (2014).
[7] H. Wang, J. Qin, X. Ding, M.-C. Chen, S. Chen, X. You, Y.-M. He, X. Jiang, L. You, Z. Wang, C. Schneider, J. J. Renema, S. Höfling, C.-Y. Lu, and J.-W. Pan, Boson Sampling with 20 Input Photons and a 60-Mode Interferometer in a 10^{14}-Dimensional Hilbert Space, Phys. Rev. Lett. **123**, 250503 (2019).
[8] J. Arrazola, V. Bergholm, K. Bradler, T. Bromley, M. Collins, I. Dhand, A. Fumagalli, T. Gerrits, A. Goussev, L. Helt *et al.*, Quantum circuits with many photons on a programmable nanophotonic chip, Nature (London) **591**, 54 (2021).
[9] D. J. Brod, E. F. Galvao, A. Crespi, R. Osellame, N. Spagnolo, and F. Sciarrino, Photonic implementation of boson sampling: A review, Adv. Photon. **1**, 034001 (2019).

[10] E. Knill, R. Laflamme, and G. J. Milburn, A scheme for efficient quantum computation with linear optics, Nature (London) **409**, 46 (2001).
[11] P. Kok, W. J. Munro, K. Nemoto, T. C. Ralph, J. P. Dowling, Jonathan, and G. J. Milburn, Linear optical quantum computing with photonic qubits, Rev. Mod. Phys. **79**, 135 (2007).
[12] I. L. Chuang, D. W. Leung, and Y. Yamamoto, Bosonic quantum codes for amplitude damping, Phys. Rev. A **56**, 1114 (1997).
[13] D. Gottesman, A. Kitaev, and J. Preskill, Encoding a qubit in an oscillator, Phys. Rev. A **64**, 012310 (2001).
[14] M. Mirrahimi, Z. Leghtas, V. V. Albert, S. Touzard, R. J. Schoelkopf, L. Jiang, and M. H. Devoret, Dynamically protected cat-qubits: A new paradigm for universal quantum computation, New J. Phys. **16**, 045014 (2014).
[15] M. H. Michael, M. Silveri, R. T. Brierley, V. V. Albert, J. Salmilehto, L. Jiang, and S. M. Girvin, New Class of Quantum Error-Correcting Codes for a Bosonic Mode, Phys. Rev. X **6**, 031006 (2016).
[16] N. Ofek, A. Petrenko, R. Heeres, P. Reinhold, Z. Leghtas, B. Vlastakis, Y. Liu, L. Frunzio, S. M. Girvin, L. Jiang, M. Mirrahimi, M. H. Devoret, and R. J. Schoelkopf, Extending the lifetime of a quantum bit with error correction in superconducting circuits, Nature (London) **536**, 441 (2016).
[17] L. Hu, Y. Ma, W. Cai, X. Mu, Y. Xu, W. Wang, Y. Wu, H. Wang, Y. P. Song, C.-L. Zou, S. M. Girvin, L.-M. Duan, and L. Sun, Quantum error correction and universal gate set operation on a binomial bosonic logical qubit, Nat. Phys. **15**, 503 (2019).
[18] P. Campagne-Ibarcq, A. Eickbusch, S. Touzard, E. Zalys-Geller, N. E. Frattini, V. V. Sivak, P. Reinhold, S. Puri, S. Shankar, R. J. Schoelkopf, L. Frunzio, M. Mirrahimi, and M. H. Devoret, Quantum error correction of a qubit encoded in grid states of an oscillator, Nature (London) **584**, 368 (2020).
[19] C. Flühmann, T. L. Nguyen, M. Marinelli, V. Negnevitsky, K. Mehta, and J. P. Home, Encoding a qubit in a trapped-ion mechanical oscillator, Nature (London) **566**, 513 (2019).
[20] M. Reck, A. Zeilinger, H. J. Bernstein, and P. Bertani, Experimental Realization of Any Discrete Unitary Operator, Phys. Rev. Lett. **73**, 58 (1994).
[21] M. Keller, B. Lange, K. Hayasaka, W. Lange, and H. Walther, Continuous generation of single photons with controlled waveform in an ion-trap cavity system, Nature (London) **431**, 1075 (2004).
[22] P. B. R. Nisbet-Jones, J. Dilley, D. Ljunggren, and A. Kuhn, Highly efficient source for indistinguishable single photons of controlled shape, New J. Phys. **13**, 103036 (2011).
[23] S. Ritter, C. Nolleke, C. Hahn, A. Reiserer, A. Neuzner, M. Uphoff, M. Mucke, E. Figueroa, J. Bochmann, and G. Rempe, An elementary quantum network of single atoms in optical cavities, Nature (London) **484**, 195 (2012).
[24] K. Hammerer, A. S. Sørensen, and E. S. Polzik, Quantum interface between light and atomic ensembles, Rev. Mod. Phys. **82**, 1041 (2010).
[25] Y. Yin, Y. Chen, D. Sank, P. J. J. O'Malley, T. C. White, R. Barends, J. Kelly, E. Lucero, M. Mariantoni, A. Megrant, C. Neill, A. Vainsencher, J. Wenner, A. N. Korotkov, A. N. Cleland, and J. M. Martinis, Catch and Release of Microwave Photon States, Phys. Rev. Lett. **110**, 107001 (2013).
[26] M. Pierre, I. Svensson, S. R. Sathyamoorthy, G. Johansson, and P. Delsing, Storage and on-demand release of microwaves using superconducting resonators with tunable coupling, Appl. Phys. Lett. **104**, 232604 (2014).
[27] M. Pechal, L. Huthmacher, C. Eichler, S. Zeytinoglu, A. A. Abdumalikov, Jr., S. Berger, A. Wallraff, and S. Filipp, Microwave-Controlled Generation of Shaped Single Photons in Circuit Quantum Electrodynamics, Phys. Rev. X **4**, 041010 (2014).
[28] E. Flurin, N. Roch, J. D. Pillet, F. Mallet, and B. Huard, Superconducting Quantum Node for Entanglement and Storage of Microwave Radiation, Phys. Rev. Lett. **114**, 090503 (2015).
[29] R. Andrews, A. Reed, K. Cicak, J. Teufel, and K. Lehnert, Quantum-enabled temporal and spectral mode conversion of microwave signals, Nat. Commun. **6**, 10021 (2015).
[30] F. Wulschner *et al.*, Tunable coupling of transmission-line microwave resonators mediated by an rf squid, Eur. Phys. J. Quantum Technol. **3**, 10 (2016).
[31] W. Pfaff, C. J. Axline, L. D. Burkhart, U. Vool, P. Reinhold, L. Frunzio, L. Jiang, M. H. Devoret, and R. J. Schoelkopf, Controlled release of multiphoton quantum states from a microwave cavity memory, Nat. Phys. **13**, 882 (2017).
[32] A. Bienfait, K. J. Satzinger, Y. Zhong, H.-S. Chang, M.-H. Chou, C. R. Conner, É. Dumur, J. Grebel, G. A. Peairs, R. G. Povey, and A. N. Cleland, Phonon-mediated quantum state transfer and remote qubit entanglement, Science **364**, 368 (2019).
[33] R. Dassonneville, R. Assouly, T. Peronnin, P. Rouchon, and B. Huard, Number-Resolved Photocounter for Propagating Microwave Mode, Phys. Rev. Appl. **14**, 044022 (2020).
[34] K. M. Sliwa, M. Hatridge, A. Narla, S. Shankar, L. Frunzio, R. J. Schoelkopf, and M. H. Devoret, Reconfigurable Josephson Circulator/Directional Amplifier, Phys. Rev. X **5**, 041020 (2015).
[35] J. Kerckhoff, K. Lalumiere, B. J. Chapman, A. Blais, and K. W. Lehnert, On-Chip Superconducting Microwave Circulator from Synthetic Rotation, Phys. Rev. Appl. **4**, 034002 (2015).
[36] B. J. Chapman, E. I. Rosenthal, J. Kerckhoff, B. A. Moores, L. R. Vale, J. A. B. Mates, G. C. Hilton, K. Lalumiere, A. Blais, and K. W. Lehnert, Widely Tunable On-Chip Microwave Circulator for Superconducting Quantum Circuits, Phys. Rev. X **7**, 041043 (2017).
[37] F. Lecocq, L. Ranzani, G. A. Peterson, K. Cicak, R. W. Simmonds, J. D. Teufel, and J. Aumentado, Nonreciprocal Microwave Signal Processing with a Field-Programmable Josephson Amplifier, Phys. Rev. Appl. **7**, 024028 (2017).
[38] S. Masuda, S. Kono, K. Suzuki, Y. Tokunaga, Y. Nakamura, and K. Koshino, Nonreciprocal microwave transmission based on Gebhard-Ruckenstein hopping, Phys. Rev. A **99**, 013816 (2019).
[39] Y.-Y. Wang, S. van Geldern, T. Connolly, Y.-X. Wang, A. Shilcusky, A. McDonald, A. A. Clerk, and C. Wang, Low-Loss Ferrite Circulator as a Tunable Chiral Quantum System, Phys. Rev. Appl. **16**, 064066 (2021).

[40] P. Lodahl, S. Mahmoodian, S. Stobbe, P. Schneeweiss, J. Volz, A. Rauschenbeutel, H. Pichler, and P. Zoller, Chiral quantum optics, Nature (London) **541**, 473 (2017).
[41] P.-O. Guimond, B. Vermersch, M. L. Juan, A. Sharafiev, G. Kirchmair, and P. Zoller, A unidirectional on-chip photonic interface for superconducting circuits, npj Quantum Inf. **6**, 32 (2020).
[42] N. Gheeraert, S. Kono, and Y. Nakamura, Programmable directional emitter and receiver of itinerant microwave photons in a waveguide, Phys. Rev. A **102**, 053720 (2020).
[43] B. Kannan *et al.*, On-demand directional photon emission using waveguide quantum electrodynamics, Nat. Phys., 10.1038/s41567-022-01869-5 (2023).
[44] C. W. Gardiner and M. J. Collett, Input and output in damped quantum systems: Quantum stochastic differential equations and the master equation, Phys. Rev. A **31**, 3761 (1985).
[45] C. W. Gardiner and P. Zoller, *Quantum Noise* (Springer, Berlin, 2004).
[46] See Supplemental Material at http://link.aps.org/supplemental/10.1103/PhysRevLett.130.050801 for a derivation of the initial model and the main analytic results and for additional details on the numerical simulations, which includes the additional Refs. [47–49].
[47] P. Kurpiers, T. Walter, P. Magnard, Y. Salathe, and A. Wallraff, Characterizing the attenuation of coaxial and rectangular microwave-frequency waveguides at cryogenic temperatures, Eur. Phys. J. Quantum Technol. **4**, 8 (2017).
[48] P. Magnard, S. Storz, P. Kurpiers, J. Schär, F. Marxer, J. Lütolf, T. Walter, J.-C. Besse, M. Gabureac, K. Reuer, A. Akin, B. Royer, A. Blais, and A. Wallraff, Microwave Quantum Link between Superconducting Circuits Housed in Spatially Separated Cryogenic Systems, Phys. Rev. Lett. **125**, 260502 (2020).
[49] M.-A. Lemonde, S. Meesala, A. Sipahigil, M. J. A. Schuetz, M. D. Lukin, M. Loncar, and P. Rabl, Phonon Networks with Silicon-Vacancy Centers in Diamond Waveguides, Phys. Rev. Lett. **120**, 213603 (2018).
[50] J. I. Cirac, P. Zoller, H. J. Kimble, and H. Mabuchi, Quantum State Transfer and Entanglement Distribution Among Distant Nodes in a Quantum Network, Phys. Rev. Lett. **78**, 3221 (1997).
[51] K. Jähne, B. Yurke, and U. Gavish, High-fidelity transfer of an arbitrary quantum state between harmonic oscillators, Phys. Rev. A **75**, 010301(R) (2007).
[52] K. Stannigel, P. Rabl, A. S. Sorensen, M. D. Lukin, and P. Zoller, Optomechanical transducers for quantum-information processing, Phys. Rev. A **84**, 042341 (2011).
[53] A. N. Korotkov, Flying microwave qubits with nearly perfect transfer efficiency, Phys. Rev. B **84**, 014510 (2011).
[54] Z.-L. Xiang, M. Zhang, L. Jiang, and P. Rabl, Intracity Quantum Communication via Thermal Microwave Networks, Phys. Rev. X **7**, 011035 (2017).
[55] B. Vermersch, P. O. Guimond, H. Pichler, and P. Zoller, Quantum State Transfer via Noisy Photonic and Phononic Waveguides, Phys. Rev. Lett. **118**, 133601 (2017).
[56] H. Ai, Y.-Y. Fang, C.-R. Feng, Z. Peng, and Z.-L. Xiang, Multinode State Transfer and Nonlocal State Preparation via a Unidirectional Quantum Network, Phys. Rev. Appl. **17**, 054021 (2022).
[57] M. A. Nielsen, A simple formula for the average gate fidelity of a quantum dynamical operation, Phys. Lett. A **303**, 249 (2002).
[58] L. H. Pedersen, N. M. Møller, and K. Mølmer, Fidelity of quantum operation, Phys. Lett. A **367**, 47 (2007).
[59] W. Chen, Y. Lu, S. Zhang, K. Zhang, G. Huang, M. Qiao, X. Su, J. Zhang, J. Zhang, L. Banchi, M. S. Kim, and K. Kim, Scalable and programmable phononic network with trapped ions, arXiv:2207.06115.
[60] C. Robens, I. Arrazola, W. Alt, D. Meschede, L. Lamata, E. Solano, and A. Alberti, Boson sampling with ultracold atoms, arXiv:2208.12253.